Polymer Chemistry

Accepted Manuscript

ROYAL SOCIETY OF CHEMISTRY

www.rsc.org/polymers

Trehalose-functionalized block copolymers form serum-stable micelles

Swapnil R Tale, Ligeng Yin, Theresa M. Reineke*

Department of Chemistry, University of Minnesota, Minneapolis, Minnesota - 55455, USA

* To whom correspondence should be addressed: treineke@umn.edu

Abstract:

Well-defined amphiphilic diblock terpolymers of poly(ethylene-*alt*-propylene)−poly[(N,N'-dimethylacrylamide)-*grad*-poly(6-deoxy-6-methacrylamido trehalose)] (denoted as PEP-poly(DMA-*grad*-MAT, or PT) have been synthesized using a PEP macromolecular chain transfer agent by reversible addition−fragmentation chain transfer (RAFT) polymerization. The content of MAT was varied from 5 to 14 mole percent in the hydrophilic block of the amphiphilic polymers yielding a family of diblock terpolymers. The reactivity ratios of DMA and trimethyl silyl protected MAT were determined to be $r_1 = 0.09 \pm 0.01$ and $r_2 = 1.6 \pm 0.1$ and thus, the hydrophilic block was a gradient copolymer consisting of a higher DMA ratio (closer to the PEP) that was terminated with a higher MAT ratio. The silyl groups were subsequently deprotected and micellar dispersions were prepared by two different techniques: nanoprecipitation (NP) and direct dissolution (DD). Micelles formed by the two methods were characterized by dynamic light scattering (DLS) and cryo-transmission electron microscopy (cryo-TEM). These PT diblock terpolymers self-assembled into spherical nanostructures in aqueous media with hydrodynamic radii of ca. 16 nm in the dispersions formed by nanoprecipitation. Micellar dispersions with greater MAT content (11 mole percent in the

hydrophilic block) exhibited sufficient contrast in cryoTEM images and the corona were clearly seen as gray halos around the micellar cores. The stability of each micellar dispersion in different biological media was examined over a period of 14 h using DLS. These results indicated that micellar dispersions are stable in 100 percent fetal bovine serum (FBS), which offers promise for *in vivo* actives delivery applications.

Introduction:

Amphiphilic block copolymers are known to assemble into micelles that are of high interest for actives delivery applications. For example, micellar systems aid in improving aqueous solubility of hydrophobic drugs via encapsulation within the micelle core.[1] For systemic delivery, the payload must be transported intact to the target site. For tumors, one method is via passive targeting known as the enhanced permeability and retention (EPR) effect.[2, 3] While in circulation, polymer-based micelle carriers encounter numerous biological barriers. Therefore, in vivo delivery systems should possess hydrophilic regions that shield their payload from non-specific interactions with serum proteins, aggregation, and clearance by the reticuloendothelial system (RES) to increase circulation lifetime.[4] Polymeric micelles can also lose their payload upon dilution. Biologically, premature release and aggregation can provoke severe side effects, including an acute immunological response,[5] signifying the need to examine the stability and aggregation behavior of micelles *in vitro*.[6]

Polyethylene glycol (PEG) is a widely studied polymer for the design of non-immunogenic carriers. A PEG hydrophilic shell has been shown to prevent aggregation and RES clearance of micelle-based carriers.[7] PEGylated nanoparticles exhibit a drastic increase in blood circulation time, higher stability of formulation upon storage, and reduced renal filtration.[8] In addition, the chemical modification of PEG is generally straightforward due its versatile

solubility in both aqueous and organic solvents. Considering these advantages, PEG does not have a well-characterized biodegradation pathway and in some cases, has been shown to cause hypersensitive reactions upon oral, dermal, and intravenous administration.[9] For these reasons, other polymers that stabilize colloidal particles from aggregation with other added benefits such as targeting are of potential interest to the biomaterials community. In one approach, Mancini, *et.al* demonstrated that trehalose glycopolymers, when covalently attached to proteins, helps retain protein activity and significantly increases the stability towards lyophilization.[10] Our lab has also examined trehalose polymers for nucleic acid delivery; Sizovs, *et. al.* showed that cationic polytrehalose block copolymers assemble with siRNA in a core (cationic block + siRNA) shell (polytrehalose) structure, which aids colloidal stability and glioblastoma cells internalization of the resulting polyplexes.[11] Carbohydrates also have the added benefit of offering receptor recognition. For example, K.Yasugi, *et. al*. formulated polymeric micelles with a glucose or galactose residue on their surface offering a sugar-bearing poly(ethylene glycol)-poly(D,L-lactide) [PEG-PLA] block copolymer. In that study, the galactose-bearing PEG−PLA micelles were shown to selectively attach to the RCA-1 lectin, which is known to recognize D-galactose residues.[12] These and related strategies may help develop intelligent micelles for receptor-mediated endocytosis, while maintaining hydrophilic shells to prevent aggregation. Thus, there exists a need to investigate synthetic approaches to install carbohydrates as hydrophilic components in assembled nanosystems such as polymeric micelles.

Herein, we explore a terpolymer design containing polymerized trehalose moieties within the hydrophilic shell for constructing polymeric micelles that are soluble and colloidally stable in aqueous salt and serum conditions.[13] Trehalose is a 1,1- α,α- linked disaccharide of two glucopyranose units and has interesting properties to be exploited for this purpose. This

disaccharide offers a higher glass-transition temperature than other related disaccharides,[14] which allows freeze-drying of biological macromolecules for preservation.[15] Trehalose is currently utilized in food preservation,[16] is not harmful when present in high concentrations in serum,[17] and has useful properties as an excipient and for cryopreservation for cells and organs.[18] Crow and Clegg showed that high concentrations of polyhydroxyl carbohydrates (sucrose, trehalose) in cells prevents organism dehydration.[19-21]

The first report describing trehalose-based polymers was published in 1979, where Kurita *et al*. synthesized trehalose-based polyurethanes using step polymerization. By condensing the two primary hydroxyl groups on trehalose with diisocynate monomers, carbohydrate-based linear polyurethanes were formed (it was mentioned that with this polymerization method, there was the possibility of chain branching).[22] In 1994, the same group established an efficient procedure to synthesize diamino-trehalose, which was converted to a diisothiocynate to afford polyureas with high aqueous solubility and biodegradability.[23] In 2002 and 2004, Teramoto , N. *et al*. reported the synthesis of a trehalose-based polyacetal using an acid catalyst for use as a thermoplastic.[24, 25] The step-growth synthesis of trehalose-based polymers has also been reported by our group using Huisgen (3+2) cycloaddition (click reaction); a 6,6'-diazido-6-6'-dideoxy trehalose monomer was created and reacted with dialkyne-oligoamine compounds to yield a series of polymers that were examined for plasmid DNA delivery to cells.[26, 27]

Herein, we report the synthesis of a trimethylsilyl (TMS)-protected trehalose monomer, 6-deoxy-6-methacrylamido-2,3,4,2′,3′,4′,6′-hepta-O-trimethylsilyl trehalose (TMS-MAT), for creation of amphiphilic block copolymers via RAFT polymerization. A family of polytrehalose (PT)-functionalized diblock terpolymers composed of three different units have been synthesized to create a diblock structure with distinct solubility profiles. An aliphatic hydrocarbon chain,

poly(ethylene-alt-propylene) (PEP), has been incorporated as the hydrophobic fragment and a polytrehalose-functionalized gradient block copolymerized with dimethyl acrylamide (DMA) was combined in the hydrophilic unit in the amphiphilic structure. DMA has demonstrated a wide range of solubility from aqueous to organic solvents,[28] and in the current system it serves to decrease the difference in polarity of the PEP and PT blocks. PEP (Tg= -65^{o}C) has served as a hydrophobic block to promote micelle core formation in macromolecular carriers. [29] In addition to providing a hydrophilic shell with possible stealth-like properties, [17] the polytrehalose-DMA block was added to increase the overall glass transition temperature of the synthesized diblock terpolymers. A control system lacking trehalose was also synthesized through copolymerization of a PEP macromolecular chain transfer agent (created through anionic polymerization) with DMA in a diblock fashion.[29] The PEP chain transfer agent was then used to generate a family of PT diblock terpolymers through RAFT polymerization with both DMA and TMS-MAT. The composition of TMS-MAT was varied from 0.05 to 0.14 mole fraction in the hydrophilic block of the diblock terpolymers. Reactivity ratio studies between DMA and TMS-MAT suggested that the hydrophilic block was a gradient copolymer.[30, 31] Micellar dispersions of the PT diblock terpolymers in water were prepared using both nanoprecipitation and direct dissolution techniques. The resulting nanostructures were characterized for size and stability with dynamic light scattering (DLS) and cryo-transmission electron microscopy (Cryo-TEM). The micelle structures were shown to remain stable from aggregation in a variety of media types.[32]

Results and Discussion:

Synthesis of 6-deoxy-6-methacrylamido-2,3,4,2′,3′,4′,6′-hepta-O-trimethylsilyl trehalose (TMS-MAT) (7)[11]:

The synthesis of TMS-MAT (7) was achieved in six steps according to a previously published procedure (see Supporting Information for synthetic details).[11] The first step involved breaking the *C2* symmetry of trehalose (1), which was accomplished by reacting anhydrous trehalose with iodine in the presence of triphenylphosphine in dry dimethyl formamide (DMF) at 80 °C. The crude product was taken to the next step without further purification and reacted with acetic anhydride in the presence of pyridine to yield a mixture of three products; acetylated mono-iodo trehalose, acetylated di-iodo trehalose, and acetylated trehalose. This mixture of products was purified using silica column chromatography to yield acetylated mono-iodo trehalose **(2).**[26, 33, 34] The second step involved the reaction of **(2)** with sodium azide in an S_N2 fashion in DMF at 80°C for 4 hours to yield acetylated mono-azido trehalose **(3)**, which was purified by recrystallization. Deprotection of the acetyl groups was achieved with sodium methoxide in methanol yielding **(4)**. Hydrogenation with palladium on carbon reduced the azide to the primary amine **(5)**.[34] Subsequent protection of the hydroxyls with trimethylsilyl (TMS) groups provided the TMS-protected aminotrehalose derivative **(6).** In the final step, **6** was reacted with methacryloyl chloride in DMF/dichloromethane (DCM) to yield the methacrylamide trehalose monomer **(7)** confirmed by ^{1}H NMR (Figure S1, Supporting Information).

Scheme 1. Synthesis of 6-deoxy-6-methacrylamido-2,3,4,2′,3′,4′,6′-hepta-O-trimethylsilyl trehalose (TMS-MAT) (7)

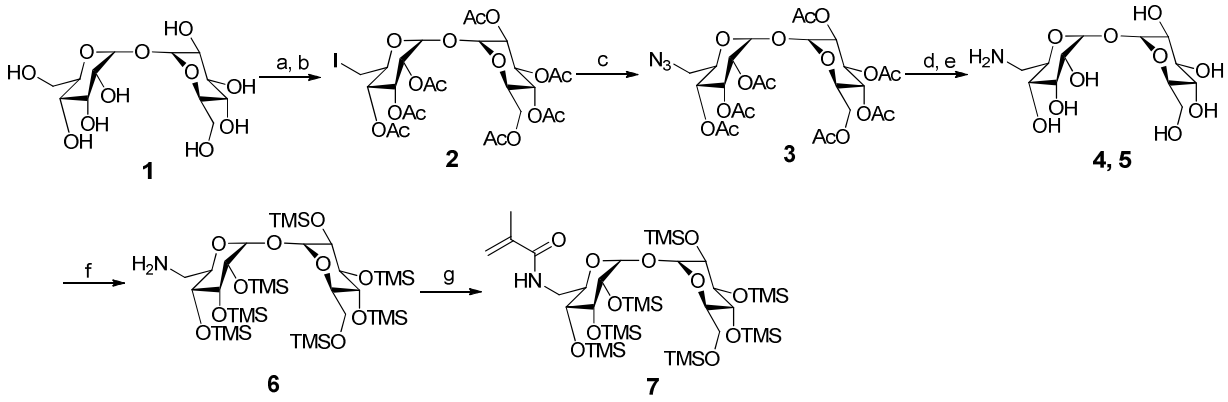

Reagents, conditions, and yields: a) I_2, PPh_3, 80°C, 4 h, b) Ac_2O, pyridine, r.t., 12 h, 20%, c) NaN_3, DMF, 80°C, 4 h, 82%, d) MeONa, MeOH, r.t., 3 h, e) H_2, Pd(C), MeOH, r.t., 20 h, 70 %, f) TMSCl, pyridine, r.t., 15 h, 90%, g) methacryloyl chloride, DMF, CH_2Cl_2, Et_3N, r.t., 4 h, quantitative.

Reactivity ratios of DMA and TMS-MAT by Non-linear Fitting:

The reactivity ratios for the copolymerization of DMA and TMS-MAT were studied in toluene at 70°C using AIBN as the initiator by free radical polymerization (Scheme S1, Supporting Information). We varied the monomer feed (mole fraction) of TMS-MAT (monomer 1) from 0.11 to 0.91 and ran seven experimental runs to calculate the reactivity ratios of copolymerization. The conversions of each monomer were kept less than 20 percent, in order to maintain the monomer feed composition during polymerization. These results are tabulated in Table S2 (Supporting Information).

We used a non-linear fitting model to analyze the reactivity ratios for copolymerization of TMS-MAT and DMA. Using the equation $F_1 = (r_1 f_1^2 + f_1 f_2) / (r_1 f_1^2 + 2 f_1 f_2 + r_2 f_2^2)$, the data was fit and calculated to be $r_1 = 0.09 \pm 0.01$ and $r_2 = 1.6 \pm 0.1$. Figure 1 shows the non-linear fit used to determine the reactivity ratios.[30, 35]

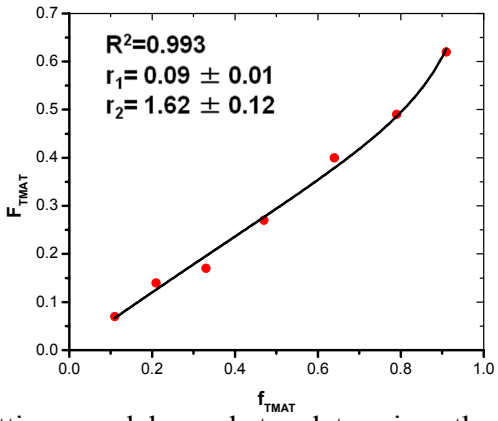

Figure 1. The non-linear fitting model used to determine the reactivity ratios for the copolymerization of TMS-MAT (monomer 1) and DMA (monomer 2). Seven experimental runs were carried out in toluene at 70°C using AIBN as the initiator.

The reactivity ratio data (i.e. $r_1 = 0.09$) indicates that homopolymerization of TMS-MAT is exceedingly slow. We attribute this fact to the bulky TMS groups that are used to protect the trehalose monomer, whereby the propagating radical site is sterically hindered. The reactivity ratio ($r_1 r_2 = 0.15$) indicates that TMS-MAT and DMA can be effectively copolymerized, however, there will be a gradual change in one monomer composition over the other. Thus, it can be concluded that the trehalose blocks are likely gradient copolymers. As polymerization proceeds, the DMA feed composition decreases due to the greater r_2. Therefore, the TMS-MAT monomer will be added towards the end of the hydrophilic block of each of the diblock terpolymers.

Synthesis of Poly (ethylene-*alt*-propylene)−poly[(*N*,*N*-dimethylacrylamide)-*grad*-poly(6-deoxy-6-methacrylamido trehalose)] (PEP-poly(DMA-*grad*-MAT)

Scheme 2. Synthesis of PT Diblock Terpolymers

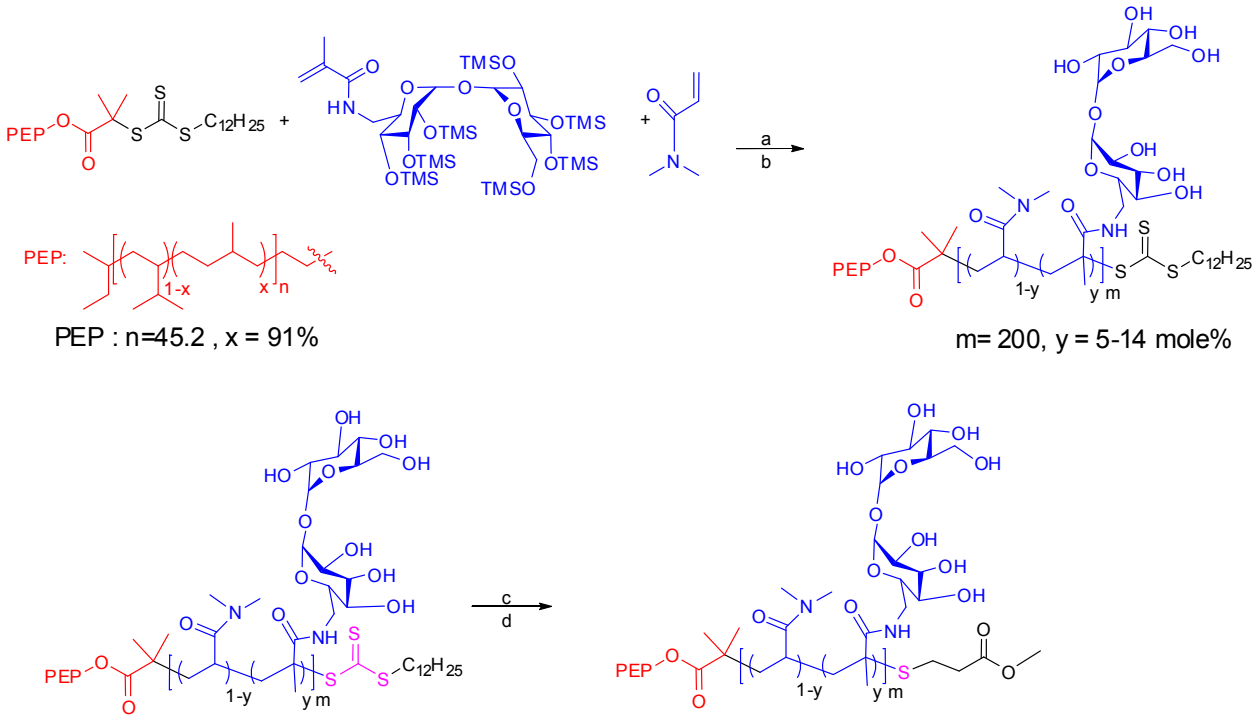

Reagents and conditions: a) AIBN, Toluene, 70°C, b) HCl in methanol, r.t., 5 min., c) n- butyl amine, TCEP, THF/methnol, 25°C, 24 h., d) methyl acrylate, r.t., 24 h.

The macromolecular chain transfer agent, PEP-CTA, was synthesized as reported in the literature.[29, 32] The number-average molar mass (M_n) of the PEP-CTA was 3.6 kg mol^{-1} (by end-group analysis in ^{1}H NMR spectroscopy), and the dispersity (□) was 1.05 (by SEC, relative to PS standards). [36] Three PT diblock terpolymers were prepared by copolymerizing DMA and TMS-MAT in toluene at 70°C using AIBN as an initiator. Characterization details (M_n and $Đ$) of the PT diblock terpolymers are shown in Table 1. SEC chromatograms of the PEP-CTA, PEP-DMA, and PT (3.6-24.5-0.11) polymers (Figure S3, Supporting Information) revealed

monomodal elution curves (Table 1). As previously discussed, the reactivity ratios of TMS-MAT (monomer 1) and DMA (monomer 2) were found to be r_1= 0.09 and r_2 = 1.59 by free radical polymerization using the non linear as well as the linear Fineman and Ross fitting model (Table S1, Table S2, and Figure S6). Based on these ratios, we believe the TMS-MAT blocks are gradient in nature. The obtained reactivity ratio data was compared with the DMA and TMS-MAG pair, and found to be similar to the published results by Yin et.al. for the DMA and TMS-glucose monomer pair.[32] TMS deprotection was achieved using HCl in methanol to yield amphiphilic diblock terpolymers (synthetic details are available in the Supporting Information). Finally, the trithiocarbonate RAFT fragment was removed by aminolysis, and complete removal was supported by UV-Vis spectroscopy (Figure S4, Supporting Information). The glass transition temperature of the amphiphilic polymers and observed increase in glass transition temperature with increasing content of MAT was determined using DSC.

Table 1. Experimental details of RAFT copolymerizations with DMA and TMS-MAT to obtain PD and PT diblock terpolymers with different compositions. The molecular weight of the PEP-CTA was 3.6 kg/mol in all cases (mass includes the $C_{12}H_{25}$ RAFT fragment).

Sample[a]	[AIBN] : [PEP-CTA]: [DMA] : [TMS-TMAT][b]	[M_0]	Time (hr)	Conv. of DMA[c]	Conv. of TMS-MAT[c]	M_n kg/ mole[d]	$Đ$[e]
PD (3.6 -23.5)	0.05 : 1 : 199 : 0	4.5	4.3	99.5%	0	23.5	1.13
PT (3.6 -21.1 -0.05)	0.05 : 1: 174.8 : 9.2	1.67	6	92%	92%	24.7	1.19
PT (3.6 -24.5 -0.11)	0.05 : 1: 179.1 : 18.3	1.68	10	99.5%	91.5%	28.1	1.23
PT (3.6 -26.4-0.14)	0.05 : 1 : 158.1 : 26.1	1.7	10	93%	87%	30.0	1.28

[a] The first value in parentheses indicates number average molecular weight of PEP in kg/mole (hydrophobic component of diblock terpolymers) and second value indicates number average molecular weight of the PDMA or PDMA and PMAT block in kg/mole (hydrophilic components of diblock terpolymers). The third value indicates the mole fractions of MAT (trehalose) repeat units in hydrophilic block of the terpolymers. [b] Initial composition of AIBN (initiator), PEP-CTA, and monomers in the feed. [c] Conversion of DMA and TMS-MAT as monitored by ^{1}H NMR spectroscopy. [d] Number average molecular weight of the diblock terpolymers after deprotection of TMS groups. [e] Polydispersity of diblock terpolymers before the removal of the trimethylsilyl protecting groups.

Formation of PT Terpolymer Micelles in Water

As reported in Table 1, four amphiphilic polymers were synthesized for this study: PD (3.6 – 23.5), PT (3.6 – 21.5 - 0.05), PT (3.6 – 24.5 – 0.11) and PT (3.6 – 26.4 – 0.14). The hydrophobic block (T_g = −65°C) in the terpolymer was kept small (3.2 kg/mol) to avoid complication from nonergodicity effects.[37, 38] Micellar dispersions of PT terpolymers were prepared by using both nanoprecipitation and direct dissolution methods.[32] Nanoprecipitation

was used in conjugation with dialysis against water to form micelles from PD (3.6 – 23.5), PT (3.6 – 21.5 - 0.05), and PT (3.6 – 24.5 – 0.11). PD (3.6 – 23.5) was readily soluble in THF, but we found a binary mixture of THF:methanol (15:2 v/v) to be the most suitable solvent for dissolving the synthesized terpolymers containing polytrehalose (PMAT).[32] Due to the large difference between polarity of the two blocks, we were unable to find a solvent system that dissolved PT (3.6 – 26.4 – 0.14), which had the highest PMAT content. Direct dissolution was employed to make micellar dispersions (by heating each sample to 60°C for two weeks) with PT (3.6 – 21.5 - 0.05), PT (3.6 – 24.5 – 0.11), and PT (3.6 – 26.4 – 0.14).

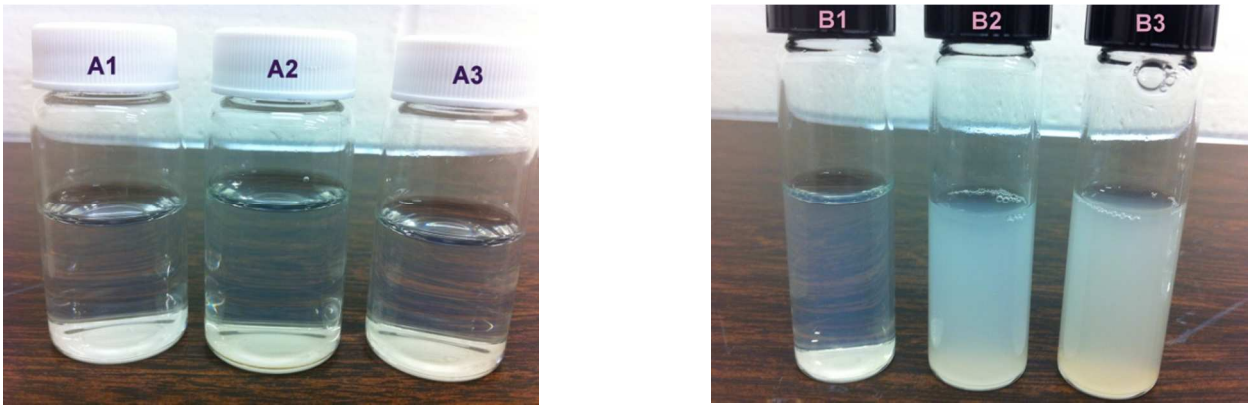

Figure 2. a) Image of micellar dispersions (1 wt percent) prepared by nanoprecipitation (NP) in water. Vial labels are as follows: A1: PD ((3.6 – 23.5), A2: PT (3.6 – 21.5 - 0.05), A3: PT (3.6 – 24.5 – 0.11). **b)** Image of micellar dispersions (1 wt percent) prepared by direct dissolution (DD) in water. Vial labels are as follows: B1: PT (3.6 – 21.5 – 0.05) B2: PT (3.6- 24.5 – 0.11) B3: PT (3.6 – 26.4 – 0.14).

Visual analysis of the samples clearly indicates that the micellar dispersions prepared by nanoprecipitation (NP) were clear and transparent with no signs of micellar aggregation. We attempted to find a solvent system that could dissolve PT (3.6 – 26.4 – 0.14) by trying different

solvent systems of THF with methanol, DMF, and DMSO but no solvent combination successfully dissolved the polymer due to the extreme differences in polarity between the hydrophilic and hydrophobic blocks. Direct dissolution (DD) was used to create micellar dispersions from all of the PT terpolymers to compare the size of the nanoparticles formed by each technique. The micellar dispersions formed by DD were white and cloudy indicating the presence of large aggregates. Micellar dispersions prepared by both techniques were first analyzed by DLS to obtain information about the average particle size and distribution in aqueous medium. Micelles formed by NP exhibited hydrodynamic radii of ca. 14 nm, with narrow dispersity in the cases of PD (3.6-23.5), PT (3.6-21.5-0.05) and PT (3.6-24.5-0.11). Large aggregates were absent according to REPES analysis (Figure 3a). The obtained results were verified with the correlation function using the cumulant expansion (Figure S7 - S9, Supporting Information). These results are tabulated in Table 2 and Figure 3a. Micelles formed by DD showed the presence of large aggregates in the case of the three PT formulations: (3.6-21.5-0.05), (3.6-24.5-0.11), and (3.6-26.4-0.14) by REPES analysis (Table 2 and Figure 3b). A double exponential correlation function was used to verify the data, which was consistent with our previous result (Figure S10 - S12). Bimodal hydrodynamic radii (R_h) of 12/52 and 21/129 nm were observed for the miceller dispersions prepared from PT (3.6-21.5-0.05) and PT (3.6-24.5-0.11) by DD, respectively. When the same diblock terpolymers were used to form micellar dispersions via the NP method, hydrodynamic radii ca. 15nm were found to be prevalent for each sample with a narrow dispersity.

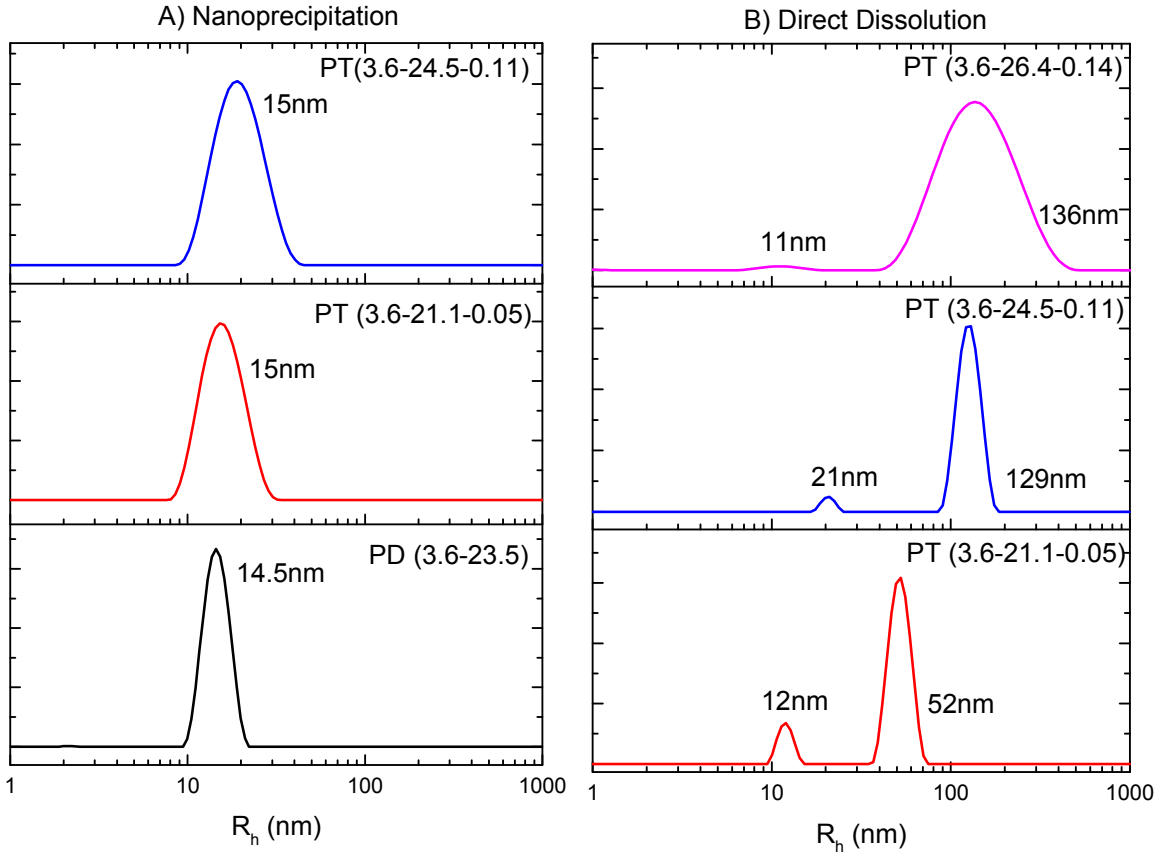

Figure 3. DLS characterization of the micellar dispersions (1 wt percent) formed by A) NP and B) DD by REPES analysis. The scattering angle was 90°. Peak positions are shown in Table 2.

Table 2. DLS Characterization of Micellar Dispersions Formed by the Terpolymers in Water

Sample	Conc.	Method	R_h1 (nm)	R_h2 (nm)
PD(3.6-23.5)[a]	1wt%	NP	14.69±0.2	
PT(3.6-21.1-0.05)[a]	1wt%	NP	14.43±0.4	
PT(3.6-24.5-0.11)[a]	1wt%	NP	14.3 ±0.2	
PT(3.6-21.1-0.05)[b]	1wt%	DD	13.6 ±0.3	55 ± 1.3
PT(3.6-24.5-0.11)[b]	1wt%	DD	21.3±0.7	129.7± 3.7
PT(3.6-26.4-0.14)[b]	1wt%	DD	16.7 ±0.4	173.9 ± 7.2

[a]A cumulant expansion function was used to determine the hydrodynamic radii by fitting the data into the correlation function. A linear regression of Γ vs. q^2 was performed over 5 angles between 60° to 120° in increments of 15° (for further information see Supporting Information Figures S7-S9). [b]A double exponential function was used to determine the hydrodynamic radii by fitting the data into the correlation function. Linear regression of Γ vs. q^2 was performed over 5 angles between 60° to 120° in increment of 15° (for further information see Supporting Information Figure S10-S12).

The T_g of each synthesized PT terpolymer was also determined; Figure S5 (Supporting Information) reveals that as more trehalose content is introduced into the hydrophilic blocks, the T_g increases. Nanoprecipitation followed by dialysis was found to be the preferred technique for these high T_g polymers to form nanostructures in solution.[39-41] (Direct dissolution technique resulted in larger aggregates).

Cryo-TEM was used to image the micelles. Figure 4 shows micrographs of the dispersions of PT (3.6-21.5-0.05) and PT (3.6-24.5-0.11) micelles in water, and both samples were shown to be spherical micelles with narrow dispersity in particle size. The micelle cores were shown as the dark circles in the images and their radii were determined to be 8 ± 1 nm in both cases. The existence of micelle coronae were revealed by grey halos around the dark cores as highlighted by black arrows in Figure 4b. Similar to our previous results with glucose-functionalized micelles,[32] the electron-rich trehalose moieties greatly enhanced the contrast of micelle coronae and made them visible even in a water-swollen state. For example, the electron density of micelle corona was calculated to be 412 e nm^{-3} in PT (3.6-24.5-0.11) micelles and 427 e nm^{-3} in PT (3.6-24.5-0.11) micelles, compared to 397 e nm^{-3} in PEP-PDMA ones and 314 e nm^{-3} of amorphous ice.[42]

a) PT (3.6-21.1-0.05) **b) PT (3.6-24.5-0.11)**

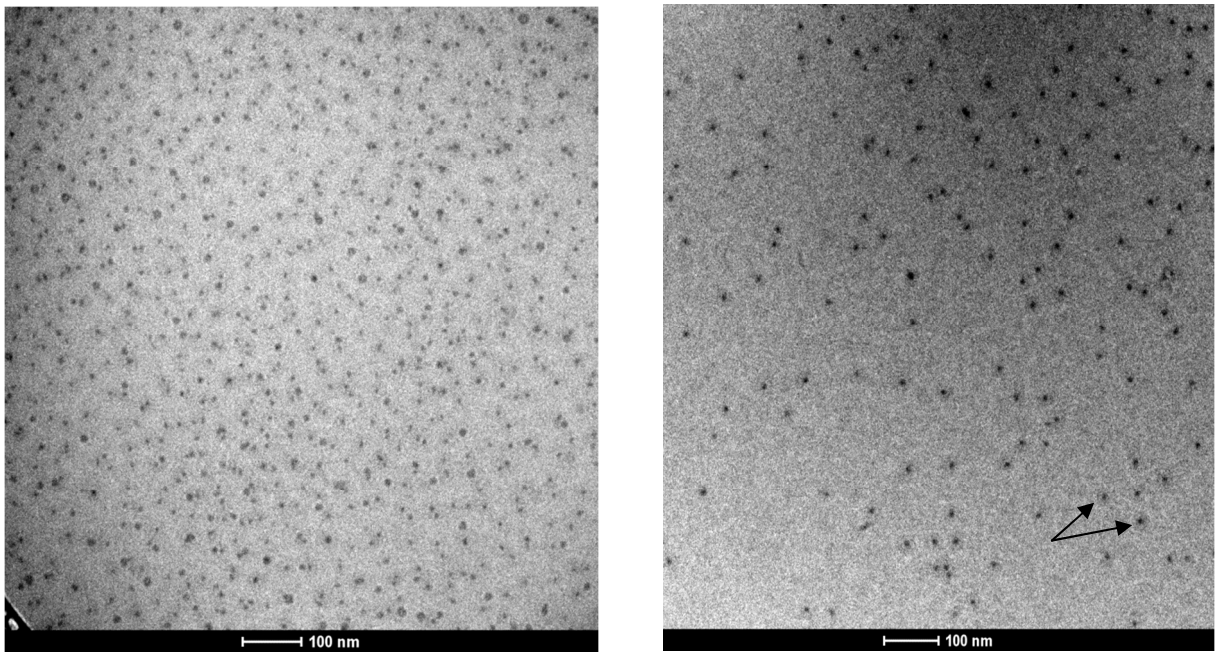

Figure 4. Cryo-TEM images of a 1 wt percent aqueous micelle dispersion formed by NP from polymers: a) PT (3.6-21.1-0.05) and b) PT (3.6-24.5-0.11). Arrows indicate the shell structure

around the dark core (presence of grey halos around the micelles due to the electron dense MAT moieties). Images were recorded on a FEI Tecnai G2 Spirit BioTWIN transmission electron microscope (TEM) at ca. –178 °C, and an accelerating voltage of 120 kV was applied onto a LaB6 emitter. No external staining was used for TEM samples.

Stability of Micelles in Biological Media

The stability of polymeric nanocarriers in biological media is critical to their use in biological applications such as drug delivery. Therefore, to gain more insight into micelle stability in biologically-relevant environments, the polytrehalose-functionalized micelles were examined by nanoprecipitation in four different biological media types (PBS, serum-free Opti-MEM, DMEM containing 10% fetal bovine serum (FBS), and 100% FBS. The stability of the PT (3.6-21.5-0.05) micelle dispersions in PBS and Opti-MEM were first examined by diluting the micellar dispersion with a 1:5 (v/v) (dispersion: media). The micellar stability from aggregation was then observed using DLS over a period of 14 hours.

As previously mentioned, REPES analysis of the micelles formed in water by NP revealed monodisperse dispersions with radii of about 15 nm, while the DD technique revealed micelle aggregation (Figure 3). Micelles were subsequently formed via NP in water, diluted with different biological media, and observed over time via DLS. Figure 5 shows the REPES distribution curves of PT (3.6-21.5-0.05) micelles at 0 and 14 hours after dilution. The micelles were found to be stable in PBS and Opti-MEM solutions over the 14 hour time period where only a slight size increase was noted (3nm) upon micelle dilution in PBS when compared to the water solutions. A cumulant expansion function was used to verify the observed data (Water, PBS and Opti-MEM), which determined that the hydrodynamic radii do not generally change (and a monomodal distribution was observed). However, when the micellar dispersion was

diluted in either DMEM containing 10% FBS or 100% FBS, a bimodal size distribution was noticed in the REPES analysis, as shown in Figure 5. Yin et. al have previously found that micelles containing glucose that are diluted in media containing serum also produces a bimodal distribution in the observed sizes with DLS.[32] That study also showed that micelles created from PDMA-PEP block copolymers also formed stable structures in biological media.[32] REPES analysis showed that the micelle peak overlapped with the FBS protein peaks (Figure 5). A double exponential analysis was performed to obtain the hydrodynamic radii as reported in Table 3. No other peaks evolved in the DLS over the period of 14 hrs (at higher sizes) nor did the peaks shift to higher sizes, which signifies that the micelles are very stable in serum-containing media and do not aggregate with serum proteins. Overall, the DLS results revealed that micelles formed by NP with the PT block copolymers show excellent stability in all of the biological media including 100% serum for up to 14 hours.

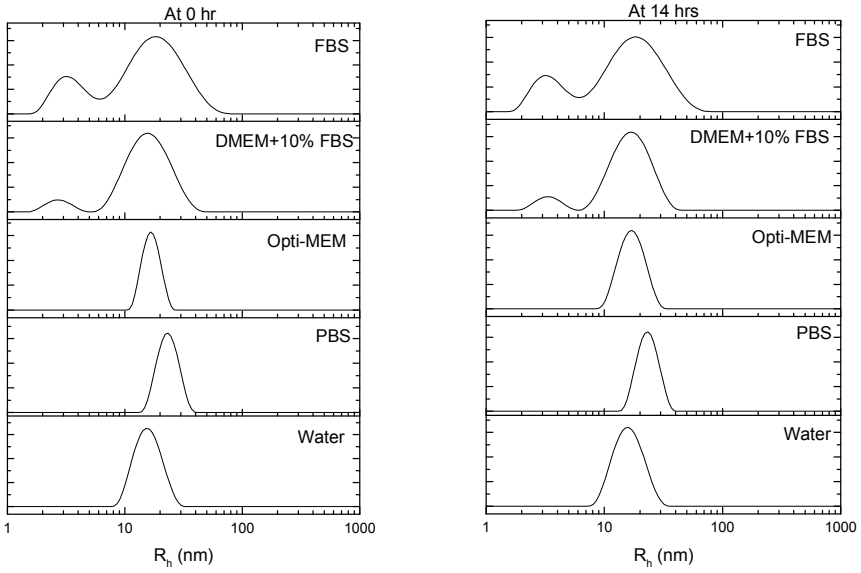

Figure 5. REPES distribution curves of PT (3.6-21.5-0.05) micelles formed by NP in water and subsequently diluted in the indicated biological media. Data were taken at time points of 0 and 14 hours following dilution. The scattering angle for the analysis was 90^o.

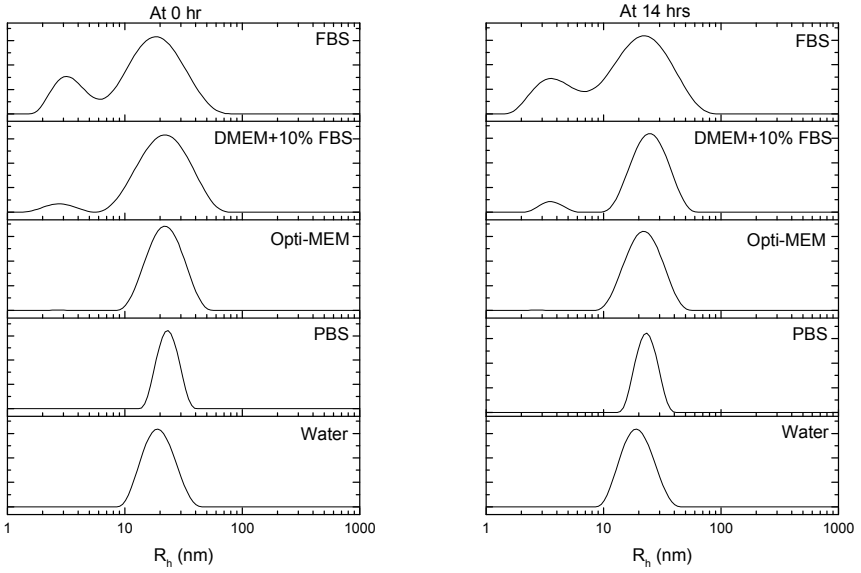

Figure 6. REPES distribution curves of PT (3.6-24.5-0.11) micelles formed by NP in water and subsequently diluted in the indicated biological media. Data were taken at time points of 0 and 14 hours following dilution. The scattering angle for the analysis was 90^o.

Table 3: Hydrodynamic radii and dispersities for PT micelles calculated after performing cumulant or double exponential expansion functions.

Samples	Time (hr)	Water[b]	PBS[b]	Opti-MEM[b]	DMEM+10% FBS[c]	100% FBC[c]
PT(3.6-21.1-0.05)	0	16.3 ± 0.1 (0.141)[d]	19.4 ± 0.1 (0.082)[d]	16.6 ± 0.7 (0.134)[d]	17.9 ± 0.3 4 ± 0.2	23.3 ± 0.2 4.1 ± 0.1
	14	15.9 ± 0.1 (0.152)[d]	17.9 ± 0.1 (0.072)[d]	16.2 ± 0.1 (0.145)[d]	17.7 ± 0.2 4 ± 0.2	21.7 ± 0.1 3.8 ± 0.1
PT(3.6-24.5-0.11)	0	19.5 ± 0.1 (0.136)[d]	22 ± 0.1 (0.068)[d]	21.2 ± 0.1 (0.147)[d]	24.2 ± 0.2 4.8 ± 0.1	23.7 ± 0.3 4.1 ± 0.1
	14	18.5 ± 0.1 (0.124)[d]	24.1 ± 0.1 (0.082)[d]	20.7 ± 0.1 (0.101)[d]	24.8 ± 0.1 5.2 ± 0.2	23.9 ± 0.1 5.7 ± 0.8

[a]Dispersions (1 weight percent) of two samples prepared by NP in water. [b] Hydrodynamic radius was calculated using a cumulant expansion function. [c] Hydrodynamic radius was calculated using a double exponential function. [d] μ/Γ^2 values at 90° scattering angle. The scattering angle was 90° for the reported Rh. Literature reported values for viscosity and refractive index for the calculation of Rh (in respective medium) were used.[32]

Conclusion

In summary, we have synthesized well-defined architectures of trehalose-functionalized, amphiphilic diblock terpolymers using a combination of RAFT and anionic polymerizations. The purpose of introducing trehalose in the polymer was to increase the difference in polarity between the hydrophilic and hydrophobic blocks, which lead to self-assembly of the micelle structures in water. The reactivity ratios determined for the MAT and DMA monomers (obtained via free radical polymerization) indicated that the hydrophilic blocks of are gradient in

nature, thus, having a higher DMA content near the PEP block and a higher trehalose content near the terpolymer end. The T_g of the PT diblock terpolymers increased as the mole percent of trehalose in the polymer backbone increased. Micelles were readily formed via NP for samples containing up to 11 mole percent of trehalose in the hydrophilic block to form micelles. DLS and cryo-TEM characterization data suggested that spherical micelles with monomodal hydrodynamic radii ca. 15 nm were observed. Micelles were also formed via DD for the sample containing the higher percentage of trehalose, PT (3.6-26.4-0.14), as micelles with this polymer were unable to be formed via NP. We also employed DD as a micelle formation method to determine the size difference between polymeric micelles formed using both techniques. The DD micelle formation technique generally revealed the formation of large aggregates. CryoTEM images revealed that the presence of trehalose was found to increase the shell contrast (grey halos around dark micelle cores) due to the electron rich MAT moieties in the diblock terpolymers. DLS analysis of the micelles indicated that these structures are stable from aggregation when incubated with a variety of salt and serum-containing media, thus, supporting further optimization of these structures for systemic drug delivery applications.

Acknowledgements

We are grateful for funding from the National Institutes of Health (NIH) Director's New Innovator Award Program (DP2OD006669-01) and to the University of Minnesota College of Science and Engineering Characterization Facility, which has received equipment funding from the NSF through the UMN MRSEC program.

Notes and references

Experimental details of the synthesis of the trehalose monomer and diblock terpolymers are reported in the electronic Supporting Information. Figures S1, S2, S3, S4, and S5 shows the

characterization of monomer and polymers by NMR, UV-VIS and DSC. Reactivity ratios data is also shown (Scheme S1, Table S1, S2 and S3 and Figure S6). DLS data is shown in Figures S7 – S12 (linear regression of Γ vs. q^2 over 5 different angles from 60° to 120° for the micelles formed by both the nanoprecipitation and direct dissolution methods).

Corresponding Author Information:

Email: treineke@umn.edu, Fax: 612-626-7541

References

1. R. Duncan, *Nat. Rev. Drug Discov.*, 2003, **2**, 347-360.
2. L. E. van Vlerken, T. K. Vyas and M. M. Amiji, *Pharm Res.*, 2007, **24**, 1405-1414.
3. H. Maeda, J. Wu, T. Sawa, Y. Matsumura and K. Hori, *J. Control. Release*, 2000, **65**, 271-284.
4. D. E. Owens and N. A. Peppas, *Int. J. Pharm.*, 2006, **307**, 93-102.
5. G. Gaucher, R. H. Marchessault and J. C. Leroux, *J. Control. Release*, 2010, **143**, 2-12.
6. T. Miller, R. Rachel, A. Besheer, S. Uezguen, M. Weigandt and A. Goepferich, *Pharm Res.*, 2012, **29**, 448-459.
7. K. Osada, R. J. Christie and K. Kataoka, *J. R. Soc. Interface*, 2009, **6** S325-S339.
8. N. Zhang, P. R. Wardwell and R. A. Bader, *Pharmaceutics*, 2013, **5**, 329-352.
9. K. Knop, R. Hoogenboom, D. Fischer and U. S. Schubert, *Angew. Chem., Int. Ed.*, 2010, **49**, 6288-6308.
10. R. J. Mancini, J. Lee and H. D. Maynard, *J. Am. Chem. Soc.*, 2012, **134**, 8474–8479.
11. A. Sizovs, L. Xue, Z. P. Tolstyka, N. P. Ingle, Y. Wu, M. Cortez and T. M. Reineke, *J. Am. Chem. Soc.*, 2013, **135**, 15417−15424.
12. K. Yasugi, T. Nakamura, Y. Nagasaki, M. Kato and K. Kataoka, *Macromolecules*, 1999, **32**, 8024-8032.
13. A. D. Elbein, Y. T. Pan, I. Pastuszak and D. Carroll, *Glycobiology*, 2003, **13**, 17R-27R.
14. J. L. Green and C. A. Angell, *J. Phys. Chem.*, 1989, **93**, 2880-2882.
15. J. H. Crowe, L. M. Crowe, J. F. Carpenter and C. A. Wistrom, *Biochem. J.*, 1987, **242**, 1-10.
16. B. Roser, *Trends Food Sci. Technol.*, 1991, **2**, 66-69.
17. N. Teramoto, N. D. Sachinvala and M. Shibata, *Molecules*, 2008, **13**, 1773-1816.
18. J. H. Crowe and L. M. Crowe, *Nat. Biotechnol.*, 2000, **18**, 145-146.
19. J. S. Clegg, P. Seitz, W. Seitz and C. F. Hazlewood, *Cryobiology*, 1982, **19**, 306-316.
20. J. S. Clegg, *Methods Enzymol.*, 1986, **127**, 230-239.
21. J. H. Crowe, L. M. Crowe and D. Chapman, *Science*, 1984, **223**, 701-703.
22. K. Kurita, N. Hirakawa, H. Morinaga and Y. Iwakura, *Makromol. Chem.*, 1979, **180**, 2769-2773.
23. K. Kurita, N. Masuda, S. Aibe, K. Murakami, S. Ishii and S. I. Nishimura, *Macromolecules*, 1994, **27**, 7544-7549.
24. N. Teramoto, Y. Arai, Y. Shibasaki and M. Shibata, *Carbohydr. Polym.*, 2004, **56**, 1-6.

25. N. Teramoto, M. Niwa and M. Shibata, *Materials*, 2010, **3**, 369-385.
26. S. Srinivasachari, Y. M. Liu, G. D. Zhang, L. E. Prevette and T. M. Reineke, *J. Am. Chem. Soc.*, 2006, **128**, 8176-8184.
27. S. Srinivasachari, Y. M. Liu, L. E. Prevette and T. M. Reineke, *Biomaterials*, 2007, **28**, 2885-2898.
28. L. R. Snyder and J. J. Kirkland, in *Introduction to Modern Liquid Chromatography, second edition*, John Wiley & Sons, New York, 1979, pp. 246-268.
29. L. Yin and M. A. Hillmyer, *Macromolecules*, 2011, **44**, 3021-3028.
30. S. S. Al-Deyab, M. H. El-Newehy and A. M. Al-Hazmi, *Molecules*, 2010, **15**, 4750-4756.
31. A. M. Brown, *Comput. Methods Programs Biomed.*, 2001, **65**, 191-200.
32. L. Yin, M. C. Dalsin, A. Sizovs, T. M. Reineke and M. A. Hillmyer, *Macromolecules*, 2012, **45**, 4322-4332.
33. T. M. Reineke and M. E. Davis, *Bioconjug. Chem.*, 2003, **14**, 247-254.
34. M. Wada, Y. Miyazawa and Y. Miura, *Polym. Chem.*, 2011, **2**, 1822-1829.
35. G. Odian, *Principles of polymerization, 4th ed.*, John Wiley & Sons, Inc., Hoboken, NJ, 2004.
36. J. T. Lai, D. Filla and R. Shea, *Macromolecules*, 2002, **35**, 6754-6756.
37. S. Jain and F. S. Bates, *Science*, 2003, **300**, 460-464.
38. S. Jain and F. S. Bates, *Macromolecules*, 2004, **37**, 1511-1523.
39. S. Pearson, N. Allen and M. H. Stenzel, *J. Polym. Sci., Part A: Polym. Chem.*, 2009, **47**, 1706−1723.
40. A. E. Smith, A. Sizovs, G. Grandinetti, L. Xue and T. M. Reineke, *Biomacromolecules,* 2011, **12**, 3015−3022.
41. S. R. S. Ting, E. H. Min, P. Escale, M. Save, L. Billon and M. H. Stenzel, *Macromolecules*, 2009, **42**, 9422−9434.

TOC image: